

Double-Slit Interference in the Ion Dynamics of Dissociative Photoionization

Pei-Lun He[✉], Karen Z. Hatsagortsyan[✉], and Christoph H. Keitel[✉]
Max-Planck-Institut für Kernphysik, Saupfercheckweg 1, 69117 Heidelberg, Germany

(Received 17 October 2022; revised 3 April 2023; accepted 13 June 2023; published 5 July 2023)

The ion momentum distribution in the x-ray-induced dissociative photoionization of molecules is investigated, treating the ionization analytically under the Born-Oppenheimer approximation and simulating numerically the ion motion via the Schrödinger equation. The ion-photoelectron entanglement transfers information of the electronic interference to the ion dynamics. As a consequence, the ion momentum distributions of dissociative molecular photoionization present Young's double-slit interference when the photoelectron emission angle is fixed. We demonstrate that double-slit interference signatures persist in the ion longitudinal momentum shift even when the information of the correlated photoelectron is lost, which is the case for heteronuclear molecules when an additional photoelectron recoil momentum arises due to the different ion masses. For the case of sequential double ionization, we show that double-slit interference in the ion dynamics can be utilized for coherent control of the molecular dynamics.

DOI: 10.1103/PhysRevLett.131.013201

The ionization of an atom or a molecule naturally generates entanglement between the photoelectron and its parent ion [1–3]. The interaction of strong laser fields with molecules enables the creation and manipulation of entangled states in the femtosecond timescale [4,5]. For single ionization, the constraint of energy-momentum conservation allows one to derive the kinetic information of the ion once the photoelectron information is known [6]. In reversal, the photoelectron momentum distribution can also be reconstructed from the ion's momentum [7]. More nontrivial entangled quantum dynamics can be observed in systems beyond two-body interaction. Single-photon double ionization is an example with clearly correlated ionization signals [8–12]. In the case of strong-field ionization, the correlation between photoelectrons and ions can lead to ultrafast thermalization in nonsequential double ionization [13–15]. The dissociative ionization of molecules [16–19] is another typical example of correlated phenomena, where photoionization is followed by molecule dissociation. It has been shown using pump-probe experiments that the entangled photoelectron could restrict the coherence of the ion dynamics [20–22]. By analyzing the joint energy spectrum, the nuclei motion and different paths of the molecule dissociation could be resolved [23–28].

The emission of the photoelectron in molecular ionization is accompanied by a recoil momentum to its parent ion,

which can excite molecules to vibrational and rotational states [29,30]. As the inner shell electron is ionized preferably when the incident photon has high energy, the recoil momentum mostly focuses on the emitter atom [31]. The nondipole effect (also called radiation pressure effect), which originates from the linear momentum of the absorbed photon, also plays a role in the subsequent dissociative dynamics by inducing an additional rotation of the ion momentum distribution [32,33]. In photoelectron dynamics of diatomic molecules, wave packets released from the two atomic sites can interfere with each other, causing double-slit interference in both single-photon [7–10,34–45] and strong-field ionization [46–49]. This two-center interference is also called Cohen-Fano interference [34]. Electron-ion entanglement [50], as demonstrated by [47], allows for the disentanglement of *gerade* and *ungerade* types of interference. The entanglement and double-slit interferences persist even at large internuclear distances [51–53]. The combination of molecular double-slit interference and the nondipole effect has interesting applications. By studying the nondipole shift of the photoelectron interference fringe, the photon traveling time through the molecular bond length has been identified [49,54–57]. For the ion dynamics, however, the effects of double-slit interference remain little explored [50,58]. Intuitively, one expects that when the entangled photoelectron emission angle is fixed, the electronic double-slit interference is recognizable in the ion momentum distribution. However, it is unclear whether observing double-slit interference in the ion dynamics is possible without coincidentally measuring the correlated photoelectron.

In this Letter, we theoretically investigate the three-body dynamics of the photoelectron and nuclei in the dissociative photoionization of diatomic molecules initiated by the

Published by the American Physical Society under the terms of the [Creative Commons Attribution 4.0 International license](#). Further distribution of this work must maintain attribution to the author(s) and the published article's title, journal citation, and DOI. Open access publication funded by the Max Planck Society.

x-ray photon absorption. We explore the possibility of observing double-slit interference in ion dynamics, with and without correlated electron information. The differential joint momentum spectrum is calculated, demonstrating Young's interference in the relative ion momentum distribution at a fixed photoelectron emission direction. The interference is transferred from the photoelectron to ion momentum due to entanglement. In the ionization of heteronuclear molecules, a nondipole recoil momentum arises due to the different ion masses. Quantifying the nondipole effect via the average of the relative nuclear momentum along the photon propagation direction, we demonstrate that double-slit interference signatures survive in the relative nuclear momentum even after the integration over the photoelectron energy and the emission angle. The essential element here is the additional nondipole recoil, which is nonvanishing only for heteronuclear molecules. Using double ionization as an example, we show that double-slit interference due to the photoelectron-ion entanglement can be utilized in the coherent control of molecule dynamics by restricting to specific photoelectron emission angles.

We investigate the interaction between a diatomic molecule in its ground state and a photon propagating along the z axis. The significant difference in mass between electrons and nuclei justifies the use of the Born-Oppenheimer approximation (BOA), which neglects higher-order corrections that are of the order $O\{(m_e/\mu)[(M_1 - M_2)/(M_1 + M_2)]\}$ [59,60]. We use perturbation theory to calculate the ionization amplitude of the molecule and numerically propagate the resulting motion of the ions using the Schrödinger equation. At the end of the propagation, the wave function is projected onto the asymptotic momentum state. Calculations of the joint transition amplitude of the photoelectron and ion yield δ functions that highlight the conservation of total momentum and energy

$$\mathbf{k}_\gamma = \mathbf{k}_e + \mathbf{P}_C, \quad (1)$$

$$\omega + W_g = \frac{\mathbf{P}^2}{2\mu} + \frac{\mathbf{P}_C^2}{2M} + \frac{\mathbf{k}_e^2}{2m_e} + \varepsilon_b, \quad (2)$$

which constrain the degrees of freedom of the inherently three-body dynamic process. Here, W_g is the molecule ground-state energy, ω the photon energy, ε_b the potential energy of the dissociated molecules, \mathbf{P} the relative momentum of the two nuclei (the direction points from nuclei 2 to nuclei 1), $M = M_1 + M_2$ the nuclei total mass, m_e the electron mass, $\mu = [M_1 M_2 / (M_1 + M_2)]$ the reduced nuclei mass, and M_1 and M_2 are the masses of the two nuclei. The transition amplitude is [61]

$$M(\mathbf{P}, \mathbf{k}_e) = \int d\mathbf{R} \chi_{\mathbf{P}}^*(\mathbf{R}) \chi_i(\mathbf{R}) T(\mathbf{k}_e; \mathbf{R}), \quad (3)$$

where $\chi_i(\mathbf{R})$ is the initial state of the nuclei, $\chi_{\mathbf{P}}(\mathbf{R})$ the final nuclei state with an asymptotic relative momentum \mathbf{P} , and the ionization amplitude $T(\mathbf{k}_e; \mathbf{R})$ is given by

$$T(\mathbf{k}_e; \mathbf{R}) = \int d\mathbf{x} \exp(-i\tilde{\mathbf{k}}_e \cdot \mathbf{x}) \frac{1}{m_e} \mathbf{k}_e \cdot \mathbf{e}_x \phi_e(\mathbf{x}; \mathbf{R}), \quad (4)$$

where $\tilde{\mathbf{k}}_e = \mathbf{k}_e - \mathbf{k}_\gamma$ is the light-front momentum [33,62,63] and $\phi_e(\mathbf{x}; \mathbf{R})$ the electronic wave function of the molecule at the relative displacement of the nuclei \mathbf{R} . The nuclei displacement \mathbf{R} plays a crucial role in electron and ion dynamics, as described by Eqs. (3) and (4). It results in electron-ion correlation and imprints the ionization information on the ion dynamics.

We first consider dissociative photoionization when the molecule has only one electron, i.e., H_2^+ and HD^+ . The ground state of the ion has an isotropic distribution. However, the emission of the photoelectron from the two nuclei has an equal probability, which results in two-path interference and yields the anisotropic ionization amplitude

$$T^{(g)}(\mathbf{k}_e; \mathbf{R}) \propto \cos\left(\frac{1}{2}\mathbf{R} \cdot \tilde{\mathbf{k}}_e\right) \exp(i\mathbf{R} \cdot \mathbf{P}^{(r)}), \quad (5)$$

where the recoil momentum $\mathbf{P}^{(r)}$, providing the initial nuclei momentum for the dissociation, is given by

$$\mathbf{P}^{(r)} = \frac{1}{2} \frac{M_1 - M_2}{M_1 + M_2} \tilde{\mathbf{k}}_e. \quad (6)$$

The structure of the ionization amplitude of Eq. (5) exhibits both double-slit interference and photoelectron recoil effects. The recoil momentum $\mathbf{P}^{(r)}$ vanishes for H_2^+ due to the identical nuclei masses.

In Fig. 1(a), we plot the joint energy spectrum (JES) of the photoelectron and the nuclei for the dissociative ionization of H_2^+ . The strip in the JES reflects energy conservation [Eq. (2)]. The peak of the photoelectron spectra is at $E_{\mathbf{k}_e}^{(m)} = \omega - I_p(\mathbf{R}_m)$ [Fig. 1(e)], where $I_p(\mathbf{R}_m)$ is the ionization energy when the nuclei displacement is $|\mathbf{R}_m| = 2$ a.u., corresponding to the peak of the ground-state nuclei distribution $|\chi_i(\mathbf{R})|^2$. After ionization, the remaining ions experience Coulomb explosion resulting in a $1/|\mathbf{R}_m|$ kinetic energy release (KER) [Fig. 1(f)].

Because of electron-ion entanglement, double-slit interference is observed in the ions' relative momentum distribution $|M(\mathbf{P}, \mathbf{k}_e)|^2$ of H_2^+ and HD^+ when the correlated photoelectron emission angle is fixed. Similar to the photoelectron, the angular oscillation shown in Fig. 1(b) arises from the double-slit interference factor $\cos(\frac{1}{2}\mathbf{R} \cdot \tilde{\mathbf{k}}_e)$ in Eq. (5). For H_2 , the dissociative ionization amplitude [61,64] is

$$T^{(u)}(\mathbf{k}_e; \mathbf{R}) \propto \sin\left(\frac{1}{2}\mathbf{R} \cdot \tilde{\mathbf{k}}_e\right) \exp(i\mathbf{R} \cdot \mathbf{P}^{(r)}), \quad (7)$$

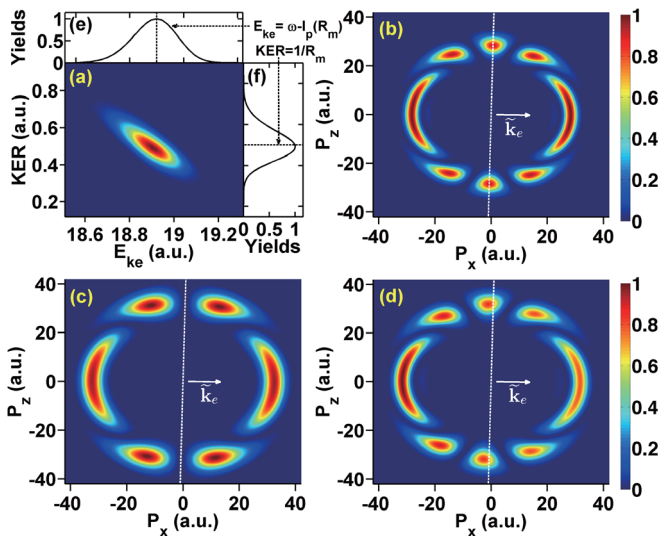


FIG. 1. Dissociative photoionization of diatomic molecules: (a) JES of the photoelectron and the nuclei of H₂⁺; panels (e) and (f) are obtained by integrating over the KER and the photoelectron energy, respectively; the ion momentum distribution of (b) H₂⁺, (c) H₂, and (d) HD⁺ when the correlated photoelectron emitting direction is $\theta_e = \pi/2$ and $\phi_e = 0$ [$\mathbf{k}_e = k_e(\sin \theta_e \cos \phi_e, \sin \theta_e \sin \phi_e, \cos \theta_e)$]. The white dashed line indicates \mathbf{R}_\perp that is perpendicular to $\tilde{\mathbf{k}}_e$. The photon energy has an energy of $\omega = 20$ a.u. and is linearly polarized along the x axis.

which results in an ion angular distribution proportional to $\sin^2(\frac{1}{2}\mathbf{R}_m \cdot \tilde{\mathbf{k}}_e)$ [Fig. 1(c)]. Note that the white dashed line in the figure represents \mathbf{R}_\perp , which is perpendicular to $\tilde{\mathbf{k}}_e$ and serves as an axis of symmetry for H₂⁺ and H₂. In the case of HD⁺, however, a nonzero recoil momentum $\mathbf{P}^{(r)}$ induces asymmetry with respect to \mathbf{R}_\perp [Fig. 1(d)]. The recoil momentum arises from the mass difference between the two nuclei. If the photoelectron is emitted from nucleus 1, the recoil momentum $-\tilde{\mathbf{k}}_e$ is focused on nucleus 1, resulting in a relative momentum shift of $-(\mu/M_1)\tilde{\mathbf{k}}_e$. Similarly, if the photoelectron is emitted from nucleus 2, the recoil momentum $-\tilde{\mathbf{k}}_e$ is focused on nucleus 2, resulting in a relative momentum shift of $(\mu/M_2)\tilde{\mathbf{k}}_e$. For isotopes, since the photoelectron has an equal probability of being released from either nucleus site, the averaged relative momentum shift is given by $\frac{1}{2}[(M_1 - M_2)/(M_1 + M_2)]\tilde{\mathbf{k}}_e$, which agrees with the recoil momentum $\mathbf{P}^{(r)}$.

The nondipole photoelectron recoil effect is more apparent in the average of the relative longitudinal momentum. Figure 2 shows the results for HD⁺ (the results for HD are similar [61]). The origin of the nonvanishing $\langle P_z \rangle$ is the recoil momentum $\mathbf{P}^{(r)}$, therefore, $\langle P_z \rangle$ vanishes for homonuclear molecules, see Eq. (6). In Figs. 2(a) and 2(b), photoelectrons with different kinetic energies are ionized from different internuclear distances \mathbf{R} . Consequently, $\langle P_z \rangle$ exhibits oscillations stemming from the double-slit

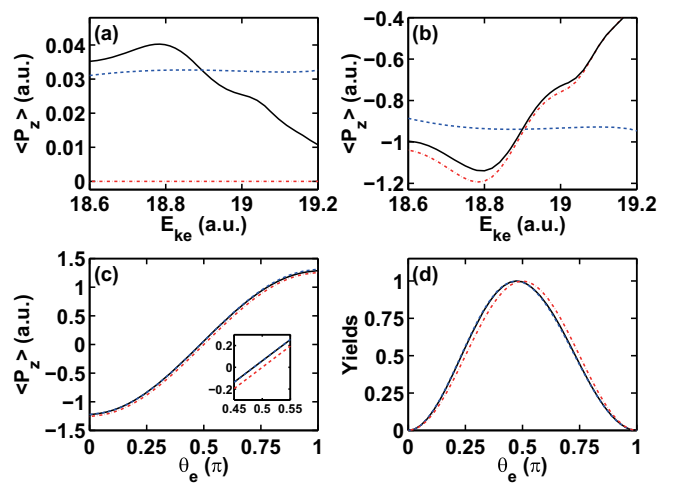


FIG. 2. The average of the relative longitudinal momentum of nuclei $\langle P_z \rangle$ of HD⁺: (a) vs the photoelectron kinetic energy at $\theta_e = \pi/2$; (b) vs the photoelectron kinetic energy at $\theta_e = \pi/4$; (c) vs the photoelectron emission angle. (d) The normalized dissociation yield integrated over the photoelectron energy. The black line utilizes the full form of $T^{(g)}(\mathbf{k}_e; \mathbf{R})$, the blue dashed line does not include the double-slit interference effect, and the red dotted-dashed line is the case with dipole approximation. The black solid and the blue dashed line overlap in panels (c) and (d). The inset shows an enlargement around $\theta_e = \pi/2$. The photon energy has an energy of $\omega = 20$ a.u. and is linearly polarized along the x axis.

interference term in Eq. (5). After integrating out the photoelectron energy, the longitudinal momentum shift persists due to the nonvanishing recoil momentum, depending on the photoelectron emission angle θ_e :

$$\langle P_z^{(\theta_e)} \rangle \approx -\frac{1}{6}(k_e \cos \theta_e - \omega/c), \quad (8)$$

with the loss of the double-slit interference signal [Fig. 2(c)]. Since $\langle P_z^{(\theta_e)} \rangle$ is primarily determined by the recoil momentum, it does not vanish even in the dipole theory (when neglecting the photon momentum) and is antisymmetric with respect to $\theta_e = \pi/2$. The nondipole effect has two competing roles here. First, it increases $\langle P_z^{(\theta_e)} \rangle$ by approximately $\frac{1}{6}(\omega/c)$, in contrast to the total nuclei momentum shift which is approximately $-\frac{3}{5}(\omega/c)$ [65]. Second, it reduces the most probable photoelectron emission angle to $\theta_e < (\pi/2)$ [Fig. 2(d)], leading to a negative contribution to the longitudinal momentum shift of the nuclei according to Fig. 2(c). As we will show below, this negative contribution dominates, causing the overall longitudinal ion momentum to be negative after integrating over all possible photoelectron emission angles.

We have shown double-slit interference in ion dynamics when the correlated photoelectron emission angle is well under control, requiring coincidence measurement experiments. The double-slit interference signature survives even

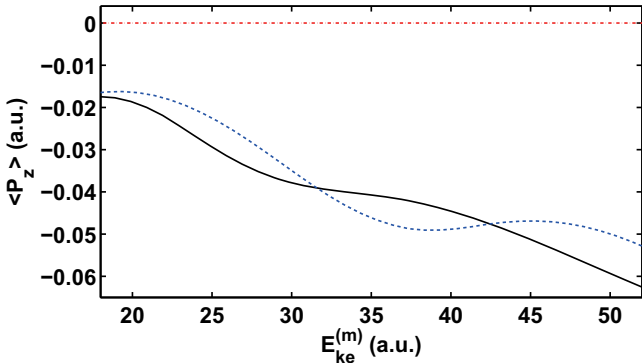


FIG. 3. The average relative longitudinal nuclei momentum $\langle P_z \rangle$ as a function of the most probable photoelectron kinetic energy $E_{ke}^{(m)} = \omega - I_p(\mathbf{R}_m)$ for HD⁺ (black solid), HD (blue dashed), and HD⁺ with the employed dipole approximation (red dotted-dashed).

if the information of the correlated electron is lost, which corresponds to integrating out the photoelectron's degree of freedom. As shown in Fig. 3, the average relative longitudinal nuclei momentum features double-slit oscillations with increasing incident photon energies. In the transverse plane, we have $\langle P_x \rangle = \langle P_y \rangle = 0$, while the absorbed photon momentum causes a nonvanishing $\langle P_z \rangle$. The negative value of $\langle P_z \rangle$ indicates that the heavier nucleus tends to be ejected in the forward direction relative to the lighter one. The nuclei momentum shift can be estimated via

$$\langle P_z \rangle \approx \frac{M_1 - M_2}{M_1 + M_2} \frac{E_{ke}}{c} \left[\frac{3}{10} \pm \frac{k_e R_m}{10} \frac{j_1(k_e R_m)}{1 \pm j_0(k_e R_m)} \right], \quad (9)$$

where the plus sign is for HD⁺, the minus sign for HD, and $j_\nu(x)$ is the spherical Bessel function of the first kind. Inheriting properties of the photoelectron momentum shift of the diatomic molecules [66], the nuclei momentum shift of Eq. (9) is also the sum of the atomic and double-slit interference contributions. The scaling of $\langle P_z \rangle$ vs the most probable photoelectron kinetic energy presented in Fig. 3 encodes valuable information on the molecular structure: the mass ratio of the two nuclei and the bond length of the molecule can be extracted from the overall slope and the oscillation of the curve.

Double-slit interference due to the photoelectron-ion entanglement can be employed in coherent control of molecular dynamics. For example, consider sequential double ionization of the HD molecule induced by pump and probe pulses. After the emission of the first electron triggered by the pump pulse, the remaining HD⁺ is in a superposition of $1s\sigma_g$ and $2p\sigma_u$ states which is further ionized by the delayed probe pulse resulting in the Coulomb explosion. The ionization amplitudes of both photoelectrons can affect the ion dynamics [61]. As a consequence of double-slit interference, the ion distribution is proportional to $\cos^2(\frac{1}{2}\mathbf{R} \cdot \tilde{\mathbf{k}}_{e_1})\cos^2(\frac{1}{2}\mathbf{R} \cdot \tilde{\mathbf{k}}_{e_2})$ for the $1s\sigma_g$ pathway

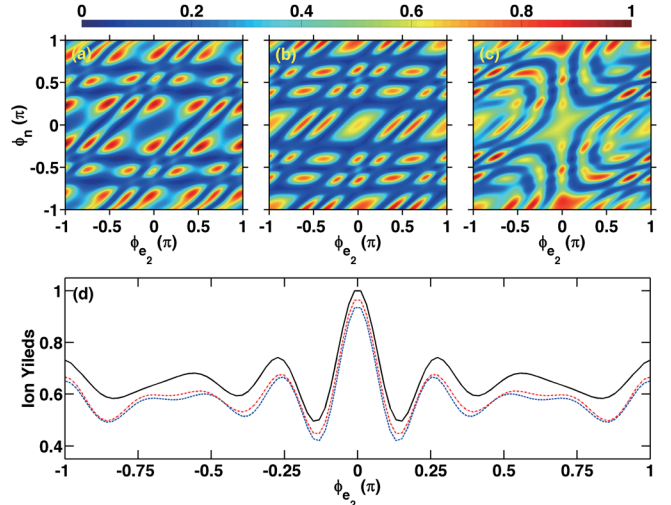


FIG. 4. (Top row) The ion angular distributions of double ionization of HD vs the photoelectron emission azimuthal angle ϕ_{e_2} when the azimuthal angle of the other photoelectron is fixed to be $\phi_{e_1} = 0$ and the time delay between the pump and probe pulses is $t_d = 1000$ a.u.: (a) the $1s\sigma_g$ pathway, (b) the $2p\sigma_u$ pathway, and (c) their coherent sum. (bottom row) The dissociation yield vs ϕ_{e_2} ($\phi_{e_1} = 0$) when the time delay is $t_d = 1000$ (black solid line), 2000 (blue dashed line), and 3000 a.u. (red dotted-dashed line). Both pump and probe pulses have the same optical frequencies of $\omega = 20$ a.u. and are circularly polarized in the x - y plane. The photoelectrons have energies $E_{ke_1} = 19.35$ a.u. and $E_{ke_2} = 18.75$ a.u., corresponding to the cases when the intermediate HD⁺ is in the $1s\sigma_g$ and $2p\sigma_u$ states, respectively; ϕ_n is the ion azimuthal angle.

[Fig. 4(a)] and $\sin^2(\frac{1}{2}\mathbf{R} \cdot \tilde{\mathbf{k}}_{e_1})\sin^2(\frac{1}{2}\mathbf{R} \cdot \tilde{\mathbf{k}}_{e_2})$ for the $2p\sigma_u$ pathway [Fig. 4(b)], where \mathbf{k}_{e_1} and \mathbf{k}_{e_2} are the momenta of the two photoelectrons. By choosing specific emission angles of the two photoelectrons, the ion distributions contributed by the two pathways could have either negligible or significant overlap [Fig. 4(c)]. When the overlap is negligible, the pathway information can be resolved via the emission angles of the entangled ion and photoelectrons. When the overlap is significant, the pathway information is lost, such that the interference is significant. Note that the overlap depends essentially on double-slit interference.

For the intermediate HD⁺, the populated $2p\sigma_u$ states are unstable and dissociate directly. Thus, Fig. 4(b) is nearly independent of the pulse time delay t_d . The populated $1s\sigma_g$ states could vibrate and rotate, resulting in the time delay dependence of Fig. 4(a). Accordingly, the dissociation yield will depend on t_d as well as the photoelectron emission angle via double-slit interference [Fig. 4(d)]. As a consequence of two-pathway interference, the ion yield is maximum when the momenta of the two photoelectrons are parallel. The recoil momentum $\mathbf{P}^{(r)}$ could induce the rotation of the intermediate HD⁺, with a rotational period $\sim(\mu|\mathbf{R}_m|/|\mathbf{P}^{(r)}|)$, resulting in the change of the photoelectron emission angle dependence of the ion yield [61].

Because of the rotation, $\phi_{e_2} = 0.7\pi$ develops to a local maximum point of the ion yield when $t_d = 3000$ a.u.. Modifications of the populated vibrational and rotational states due to double-slit interference can be monitored by scanning the ion yields as a function of t_d , similar to Refs. [21,22].

So far, we have restricted our attention to double-slit interference in ion dynamics for few-photon ionization. It is worth considering if a similar effect exists in strong-field dissociative ionization. In diatomic molecules, uphill core tunneling ionization is preferred [67,68]. Therefore, double-slit interference is absent, and the uphill core acquires most of the recoil momentum. Thus, corrections to the axial recoil approximation [17,32,69–71], which assumes the molecular axis to be along the emission direction of the nuclei at the instant of ionization, will depend on the correlated photoelectron. For rare gas dimers, the photoelectron momentum distribution in strong-field ionization can present double-slit interference [46,47,49]. Therefore, due to the electron-ion entanglement, the ion momentum distribution will also present double-slit interference when the correlated photoelectron emission angle is fixed, and the coherent control scheme discussed above applies.

In conclusion, we have demonstrated that double-slit interference can occur in the ion momentum distribution through the photoelectron-ion entanglement when the correlated photoelectron emission angle is well under control. Because of the photoelectron recoil and the ion mass difference, the longitudinal momentum shift of ions in heteronuclear molecules can be either positive or negative, depending on the photoelectron emission angle. Moreover, even when the correlated electron information is lost, the double-slit interference signature of heteronuclear molecules persists in the average longitudinal momentum shift. The interference due to the photoelectron-ion entanglement could serve as additional leverage for coherent control of molecular dynamics in dissociative photoionization. These findings can be generalized to the case of strong-field dissociative ionization.

strong-field ionization of an atomic bell-like state, arXiv: 2108.10426.

- [5] F. Shobeyri, P. Fross, H. Srinivas, T. Pfeifer, R. Moshammer, and A. Harth, Sub-femtosecond optical control of entangled states, arXiv:2110.06668.
- [6] S. Chelkowski, A. D. Bandrauk, and P. B. Corkum, Photon Momentum Sharing Between an Electron and an Ion in Photoionization: From One-Photon (Photoelectric Effect) to Multiphoton Absorption, *Phys. Rev. Lett.* **113**, 263005 (2014).
- [7] M. Schöffler *et al.*, Photo-double-ionization of H₂: Two-center interference and its dependence on the internuclear distance, *Phys. Rev. A* **78**, 013414 (2008).
- [8] D. Akoury, K. Kreidi, T. Jahnke, T. Weber, A. Staudte, M. Schöffler, N. Neumann, J. Titze, L. P. H. Schmidt, A. Czasch *et al.*, The simplest double slit: Interference and entanglement in double photoionization of H₂, *Science* **318**, 949 (2007).
- [9] K. Kreidi, D. Akoury, T. Jahnke, T. Weber, A. Staudte, M. Schöffler, N. Neumann, J. Titze, L. P. H. Schmidt, A. Czasch *et al.*, Interference in the Collective Electron Momentum in Double Photoionization of H₂, *Phys. Rev. Lett.* **100**, 133005 (2008).
- [10] M. Waitz, D. Metz, J. Lower, C. Schober, M. Keiling, M. Pitzer, K. Mertens, M. Martins, J. Viefhaus, S. Klumpp *et al.*, Two-Particle Interference of Electron Pairs on a Molecular Level, *Phys. Rev. Lett.* **117**, 083002 (2016).
- [11] M. Kircher, F. Trinter, S. Grundmann, I. Vela-Perez, S. Brennecke, N. Eicke, J. Rist, S. Eckart, S. Houamer, O. Chuluunbaatar *et al.*, Kinematically complete experimental study of Compton scattering at helium atoms near the threshold, *Nat. Phys.* **16**, 756 (2020).
- [12] M. Kircher, F. Trinter, S. Grundmann, G. Kastirke, M. Weller, I. Vela-Perez, A. Khan, C. Janke, M. Waitz, S. Zeller *et al.*, Ion and Electron Momentum Distributions from Single and Double Ionization of Helium induced by Compton Scattering, *Phys. Rev. Lett.* **128**, 053001 (2022).
- [13] X. Liu, C. F. de Morisson Faria, W. Becker, and P. Corkum, Attosecond electron thermalization by laser-driven electron recollision in atoms, *J. Phys. B* **39**, L305 (2006).
- [14] X. Liu, C. F. de Morisson Faria, and W. Becker, Attosecond electron thermalization in laser-induced nonsequential multiple ionization: Hard versus glancing collisions, *New J. Phys.* **10**, 025010 (2008).
- [15] D. Ye, M. Li, L. Fu, J. Liu, Q. Gong, Y. Liu, and J. Ullrich, Scaling Laws of the Two-Electron Sum-Energy Spectrum in Strong-Field Double Ionization, *Phys. Rev. Lett.* **115**, 123001 (2015).
- [16] I. Sánchez and F. Martín, Multichannel Dissociation in Resonant Photoionization of H₂, *Phys. Rev. Lett.* **82**, 3775 (1999).
- [17] S. Kangaparambil, V. Hanus, M. Dorner-Kirchner, P. He, S. Larimian, G. Paulus, A. Baltuška, X. Xie, K. Yamanouchi, F. He *et al.*, Generalized Phase Sensitivity of Directional Bond Breaking in the Laser-Molecule Interaction, *Phys. Rev. Lett.* **125**, 023202 (2020).
- [18] X. Gong, P. He, Q. Song, Q. Ji, K. Lin, W. Zhang, P. Lu, H. Pan, J. Ding, H. Zeng *et al.*, Pathway-resolved photoelectron emission in dissociative ionization of molecules, *Optica* **3**, 643 (2016).

*peilun@mpi-hd.mpg.de

†k.hatsagortsyan@mpi-hd.mpg.de

- [1] M. V. Fedorov, M. A. Efremov, A. E. Kazakov, K. W. Chan, C. K. Law, and J. H. Eberly, Packet narrowing and quantum entanglement in photoionization and photodissociation, *Phys. Rev. A* **69**, 052117 (2004).
- [2] S. Majorosi, M. G. Benedict, and A. Czirják, Quantum entanglement in strong-field ionization, *Phys. Rev. A* **96**, 043412 (2017).
- [3] T. Nishi, E. Löstedt, and K. Yamanouchi, Entanglement and coherence in photoionization of H₂ by an ultrashort XUV laser pulse, *Phys. Rev. A* **100**, 013421 (2019).
- [4] S. Eckart, D. Trabert, J. Rist, A. Geyer, L. P. H. Schmidt, K. Fehre, and M. Kunitski, Ultrafast preparation and

- [19] H. Liang and L.-Y. Peng, Quantitative theory for electron-nuclear energy sharing in molecular ionization, *Phys. Rev. A* **101**, 053404 (2020).
- [20] E. Goulielmakis, Z.-H. Loh, A. Wirth, R. Santra, N. Rohringer, V.S. Yakovlev, S. Zherebtsov, T. Pfeifer, A. M. Azzeer, M. F. Kling *et al.*, Real-time observation of valence electron motion, *Nature (London)* **466**, 739 (2010).
- [21] M. J. J. Vrakking, Control of Attosecond Entanglement and Coherence, *Phys. Rev. Lett.* **126**, 113203 (2021).
- [22] L.-M. Koll, L. Maikowski, L. Drescher, T. Witting, and M. J. J. Vrakking, Experimental Control of Quantum-Mechanical Entanglement in an Attosecond Pump-Probe Experiment, *Phys. Rev. Lett.* **128**, 043201 (2022).
- [23] C. B. Madsen, F. Anis, L. B. Madsen, and B. D. Esry, Multiphoton above Threshold Effects in Strong-Field Fragmentation, *Phys. Rev. Lett.* **109**, 163003 (2012).
- [24] R. E. F. Silva, F. Catoire, P. Rivière, H. Bachau, and F. Martín, Correlated Electron and Nuclear Dynamics in Strong Field Photoionization of H_2^+ , *Phys. Rev. Lett.* **110**, 113001 (2013).
- [25] J. Wu, M. Kunitski, M. Pitzer, F. Trinter, L. P. H. Schmidt, T. Jahnke, M. Magrakvelidze, C. B. Madsen, L. B. Madsen, U. Thumm, and R. Dorner, Electron-Nuclear Energy Sharing in Above-Threshold Multiphoton Dissociative Ionization of H_2 , *Phys. Rev. Lett.* **111**, 023002 (2013).
- [26] L. Yue, L. B. Madsen *et al.*, Characterization of Molecular Breakup by Very Intense Femtosecond XUV Laser Pulses, *Phys. Rev. Lett.* **115**, 033001 (2015).
- [27] W. Zhang, Z. Li, P. Lu, X. Gong, Q. Song, Q. Ji, K. Lin, J. Ma, F. He, H. Zeng *et al.*, Photon Energy Deposition in Strong-Field Single Ionization of Multielectron Molecules, *Phys. Rev. Lett.* **117**, 103002 (2016).
- [28] P. Lu, J. Wang, H. Li, K. Lin, X. Gong, Q. Song, Q. Ji, W. Zhang, J. Ma, H. Li *et al.*, High-order above-threshold dissociation of molecules, *Proc. Natl. Acad. Sci. U.S.A.* **115**, 2049 (2018).
- [29] W. Domcke and L. Cederbaum, Electronic recoil effects in high-energy photoelectron spectroscopy, *J. Electron Spectrosc. Relat. Phenom.* **13**, 161 (1978).
- [30] E. Kukk, T. D. Thomas, D. Céolin, S. Granroth, O. Travnikova, M. Berholts, T. Marchenko, R. Guillemin, L. Journel, I. Ismail, R. Püttner, M. N. Piancastelli, K. Ueda, and M. Simon, Energy Transfer into Molecular Vibrations and Rotations by Recoil in Inner-Shell Photoemission, *Phys. Rev. Lett.* **121**, 073002 (2018).
- [31] M. N. Piancastelli, T. Marchenko, R. Guillemin, L. Journel, O. Travnikova, I. Ismail, and M. Simon, Hard x-ray spectroscopy and dynamics of isolated atoms and molecules: A review, *Rep. Prog. Phys.* **83**, 016401 (2019).
- [32] M. Kircher, J. Rist, F. Trinter, S. Grundmann, M. Waitz, N. Melzer, I. Vela-Pérez, T. Mletzko, A. Pier, N. Strenger, J. Siebert, R. Janssen, L. P. H. Schmidt, A. N. Artemyev, M. S. Schöffler, T. Jahnke, R. Dörner, and P. V. Demekhin, Recoil-Induced Asymmetry of Nondipole Molecular Frame Photoelectron Angular Distributions in the Hard X-Ray Regime, *Phys. Rev. Lett.* **123**, 243201 (2019).
- [33] M. Kircher, J. Rist, F. Trinter, S. Grundmann, M. Waitz, N. Melzer, I. Vela-Pérez, T. Mletzko, A. Pier, N. Strenger, J. Siebert, R. Janssen, V. Honkimäki, J. Drnec, P. V. Demekhin, L. P. H. Schmidt, M. S. Schöffler, T. Jahnke, and R. Dörner, Photon-Momentum-Induced Molecular Dynamics in Photoionization of N_2 at $h\nu = 40$ keV, *Phys. Rev. Lett.* **123**, 193001 (2019).
- [34] H. D. Cohen and U. Fano, Interference in the photoionization of molecules, *Phys. Rev.* **150**, 30 (1966).
- [35] J. Fernández, O. Fojón, A. Palacios, and F. Martín, Interferences from Fast Electron Emission in Molecular Photoionization, *Phys. Rev. Lett.* **98**, 043005 (2007).
- [36] D. A. Horner, S. Miyabe, T. N. Rescigno, C. W. McCurdy, F. Morales, and F. Martín, Classical Two-Slit Interference Effects in Double Photoionization of Molecular Hydrogen at High Energies, *Phys. Rev. Lett.* **101**, 183002 (2008).
- [37] S. E. Canton, E. Plésiat, J. D. Bozek, B. S. Rude, P. Declava, and F. Martín, Direct observation of Young's double-slit interferences in vibrationally resolved photoionization of diatomic molecules, *Proc. Natl. Acad. Sci. U.S.A.* **108**, 7302 (2011).
- [38] D. Rolles, M. Braune, S. Cvejanović, O. Geßner, R. Hentges, S. Korica, B. Langer, T. Lischke, G. Prümper, A. Reinköster *et al.*, Isotope-induced partial localization of core electrons in the homonuclear molecule N_2 , *Nature (London)* **437**, 711 (2005).
- [39] X.-J. Liu, N. A. Cherepkov, S. K. Semenov, V. Kimberg, F. Gel'mukhanov, G. Prümper, T. Lischke, T. Tanaka, M. Hoshino, H. Tanaka, and K. Ueda, Young's double-slit experiment using core-level photoemission from N_2 : Revisiting Cohen-Fano's two-centre interference phenomenon, *J. Phys. B* **39**, 4801 (2006).
- [40] H. Sann *et al.*, Delocalization of a Vacancy Across Two Neon Atoms Bound by the van der Waals Force, *Phys. Rev. Lett.* **117**, 263001 (2016).
- [41] B. Zimmermann, D. Rolles, B. Langer, R. Hentges, M. Braune, S. Cvejanovic, O. Geßner, F. Heiser, S. Korica, T. Lischke, A. Reinköster, J. Viefhaus, R. Dörner, V. McKoy, and U. Becker, Localization and loss of coherence in molecular double-slit experiments, *Nat. Phys.* **4**, 649 (2008).
- [42] K.-J. Yuan, H. Z. Lu, and A. D. Bandrauk, Laser-induced electron diffraction in H_2 with linear and circular polarization ultrashort XUV laser pulses, *Phys. Rev. A* **80**, 061403(R) (2009).
- [43] K.-J. Yuan, H. Z. Lu, and A. D. Bandrauk, Linear-and circular-polarization photoionization angular distributions in H_2 and H_2^+ by attosecond XUV laser pulses, *Phys. Rev. A* **83**, 043418 (2011).
- [44] X. Guan, E. B. Secor, K. Bartschat, and B. I. Schneider, Double-slit interference effect in electron emission from H_2^+ exposed to x-ray radiation, *Phys. Rev. A* **85**, 043419 (2012).
- [45] M. Frolov, N. Manakov, S. Marmo, and A. F. Starace, Photodetachment of a model molecular system by an elliptically polarized field, *J. Mod. Opt.* **62**, S21 (2015).
- [46] J. Henkel, M. Lein, and V. Engel, Interference in above-threshold-ionization electron distributions from molecules, *Phys. Rev. A* **83**, 051401(R) (2011).
- [47] M. Kunitski, N. Eicke, P. Huber, J. Köhler, S. Zeller, J. Voigtsberger, N. Schlott, K. Henrichs, H. Sann, F. Trinter *et al.*, Double-slit photoelectron interference in strong-field ionization of the neon dimer, *Nat. Commun.* **10**, 1 (2019).

- [48] P.-L. He, Z.-H. Zhang, and F. He, Young's Double-Slit Interference in a Hydrogen Atom, *Phys. Rev. Lett.* **124**, 163201 (2020).
- [49] P.-L. He, K. Z. Hatsagortsyan, and C. H. Keitel, Nondipole Time Delay and Double-Slit Interference in Tunneling Ionization, *Phys. Rev. Lett.* **128**, 183201 (2022).
- [50] M. C. Tichy, F. Mintert, and A. Buchleitner, Essential entanglement for atomic and molecular physics, *J. Phys. B* **44**, 192001 (2011).
- [51] R. Mabbs, K. Pichugin, and A. Sanov, Time-resolved imaging of the reaction coordinate, *J. Chem. Phys.* **122**, 174305 (2005).
- [52] R. Mabbs, K. Pichugin, and A. Sanov, Dynamic molecular interferometer: Probe of inversion symmetry in i 2- photo-dissociation, *J. Chem. Phys.* **123**, 054329 (2005).
- [53] S. Chelkowski and A. D. Bandrauk, Visualizing electron delocalization, electron-proton correlations, and the Einstein-Podolsky-Rosen paradox during the photodissociation of a diatomic molecule using two ultrashort laser pulses, *Phys. Rev. A* **81**, 062101 (2010).
- [54] S. Grundmann, D. Trabert, K. Fehre, N. Strenger, A. Pier, L. Kaiser, M. Kircher, M. Weller, S. Eckart, L. P. H. Schmidt *et al.*, Zeptosecond birth time delay in molecular photoionization, *Science* **370**, 339 (2020).
- [55] H. Liang, S. Grundmann, Y.-K. Fang, L. Geng, Q. Gong, and L.-Y. Peng, Nondipole effects in interference patterns of a two-electron wave, *Phys. Rev. A* **104**, L021101 (2021).
- [56] K. Liu, Y. Hu, Q. Zhang, and P. Lu, Nondipole effects on the double-slit interference in molecular ionization by XUV pulses, *Opt. Express* **29**, 38758 (2021).
- [57] Z.-H. Zhang and F. He, Photoionization of H_2^+ beyond the dipole approximation with zeptosecond time resolution, *Phys. Rev. A* **103**, 033112 (2021).
- [58] J. Fernández, O. Fojón, and F. Martín, Double-slit, confinement, and non-Franck-Condon effects in photoionization of H_2 at high photon energy, *Phys. Rev. A* **79**, 023420 (2009).
- [59] I. Ben-Itzhak, E. Wells, K. D. Carnes, V. Krishnamurthi, O. L. Weaver, and B. D. Esry, Symmetry Breakdown in Ground State Dissociation of HD^+ , *Phys. Rev. Lett.* **85**, 58 (2000).
- [60] Z.-H. Zhang and F. He, Real-time calibration of nuclear velocities in the dissociation of heteronuclear molecules in strong laser fields, *Phys. Rev. A* **105**, L041104 (2022).
- [61] See Supplemental Material at <http://link.aps.org/supplemental/10.1103/PhysRevLett.131.013201> for the details. The movie shows the temporal evolution of the nuclei distribution.
- [62] P.-L. He, D. Lao, and F. He, Strong Field Theories Beyond Dipole Approximations in Nonrelativistic Regimes, *Phys. Rev. Lett.* **118**, 163203 (2017).
- [63] P.-L. He, M. Klaiber, K. Z. Hatsagortsyan, and C. H. Keitel, Nondipole coulomb sub-barrier ionization dynamics and photon momentum sharing, *Phys. Rev. A* **105**, L031102 (2022).
- [64] I. G. Kaplan and A. P. Markin, Relativistic photoeffect in the H_2 molecule, *Sov. Phys. JETP* **37**, 216 (1973), <http://www.jetp.ras.ru/cgi-bin/e/index/e/37/2/p216?a=list>.
- [65] S. Grundmann, M. Kircher, I. Vela-Perez, G. Nalin, D. Trabert, N. Anders, N. Melzer, J. Rist, A. Pier, N. Strenger, J. Siebert, P. V. Demekhin, L. P. H. Schmidt, F. Trinter, M. S. Schöffler, T. Jahnke, and R. Dörner, Observation of Photoion Backward Emission in Photoionization of He and N_2 , *Phys. Rev. Lett.* **124**, 233201 (2020).
- [66] D. Lao, P.-L. He, and F. He, Longitudinal photoelectron momentum shifts induced by absorbing a single XUV photon in diatomic molecules, *Phys. Rev. A* **93**, 063403 (2016).
- [67] T. Zuo and A. D. Bandrauk, Charge-resonance-enhanced ionization of diatomic molecular ions by intense lasers, *Phys. Rev. A* **52**, R2511 (1995).
- [68] J. Wu, M. Meckel, L. P. H. Schmidt, M. Kunitski, S. Voss, H. Sann, H. Kim, T. Jahnke, A. Czasch, and R. Dörner, Probing the tunnelling site of electrons in strong field enhanced ionization of molecules, *Nat. Commun.* **3**, 1113 (2012).
- [69] Y. Shao, P. He, M.-M. Liu, X. Sun, M. Li, Y. Deng, C. Wu, F. He, Q. Gong, and Y. Liu, Fully differential study on dissociative ionization dynamics of deuteron molecules in strong elliptical laser fields, *Phys. Rev. A* **95**, 031404(R) (2017).
- [70] A. Staudte, S. Patchkovskii, D. Pavičić, H. Akagi, O. Smirnova, D. Zeidler, M. Meckel, D. M. Villeneuve, R. Dörner, M. Y. Ivanov, and P. B. Corkum, Angular Tunneling Ionization Probability of Fixed-in-Space H_2 Molecules in Intense Laser Pulses, *Phys. Rev. Lett.* **102**, 033004 (2009).
- [71] H. Akagi, T. Otobe, A. Staudte, A. Shiner, F. Turner, R. Dörner, D. Villeneuve, and P. Corkum, Laser tunnel ionization from multiple orbitals in HCl , *Science* **325**, 1364 (2009).